EurJIC
European Journal of Inorganic Chemistry

Research Article
doi.org/10.1002/ejic.202101057

Chemistry Europe
European Chemical Societies Publishing

www.eurjic.org

Diphosphorus Release and Heterocumulene Oligomerisation by Nickel Complexes

Gabriele Hierlmeier*[a, b] and Robert Wolf*[a]

The generation of diphosphorus molecules P_2 under mild conditions in solution is a useful strategy to generate diphosphines *via* [4+2] cycloadditions. We recently described the release of P_2 units from the nickel butterfly complex [{(IMes)Ni(CO)}$_2$(μ^2,η^2:η^2-P_2)] (IMes = 1,3-bis(2,4,6-trimethylphenyl)imidazolin-2-ylidene) upon addition of CO gas. Herein, we developed an alternative protocol for the same process using heterocumulenes. In addition to formation of P_4 (the dimerisation product of P_2), the reactions afford nickel complexes of novel pincer-type ligands. Aryl isothiocyanates undergo a trimerisation within the coordination sphere of nickel and afford square planar nickel complexes with S–C–S pincer-ligand frameworks. Carbon disulfide coordinates to the [(IMes)Ni]-fragment in an η^2-fashion, affording a dinuclear complex. Similar products are formed when the N-heterocyclic carbene nickel(0) complex [(IMes)Ni(vtms)$_2$] is used as a precursor (vtms = vinyltrimethylsilane).

Introduction

The low tendency of the heavier members of the p-block elements to form multiple bonds is known as the double bond rule.[1] In the last decades, however, main group chemists have shown that this rule can be overcome, e.g. by introducing bulky substituents. A noteworthy example for this kinetic stabilisation is the isolation of a disilyne by Sekiguchi and co-workers.[2] For group 15 elements, the formation and detection of the P_2 molecule, showing a P≡P triple bond, has been investigated intensively. Diphosphorus can be stabilised in the coordination sphere of transition metal complexes.[3,4] In most of these cases P_2 acts as a ligand bridging two metal centres in an η^2-mode. Only very recently, triply bonded P≡P was stabilised in the coordination sphere of a platinum complex.[5] Upon heating white phosphorus above 1000 K, dissociation into diphosphorus occurs.[6,7] However, the conditions of this gas-phase reaction render further reactions with P_2 difficult. Therefore, several compounds which generate P_2 under milder conditions in solution have been developed (Figure 1).

The group of Cummins showed that the niobium complex **A** transfers a P_2 unit to cyclohexadiene in a Diels-Alder reaction to afford the diphosphine **B**.[8] The molecular structure was confirmed by single crystal X-ray structure analysis of a tungsten pentacarbonyl adduct of **B**. A similar [4+2]-cycloaddition was achieved by photolysis directly from P_4 in the presence of butadiene or dimethylbutadiene affording the diphosphines **B** and **C**.[9,10] Moreover, Cummins and co-workers showed that the diphosphorus bis(anthracene) compound **D** efficiently transfers P_2 to butadienes. Under mild thermal activation, **D** releases P_2 which could be detected by molecular beam mass spectrometry and ultimately transforms to red phosphorus.[11] Recently, the group of Ghadwal showed that P_2

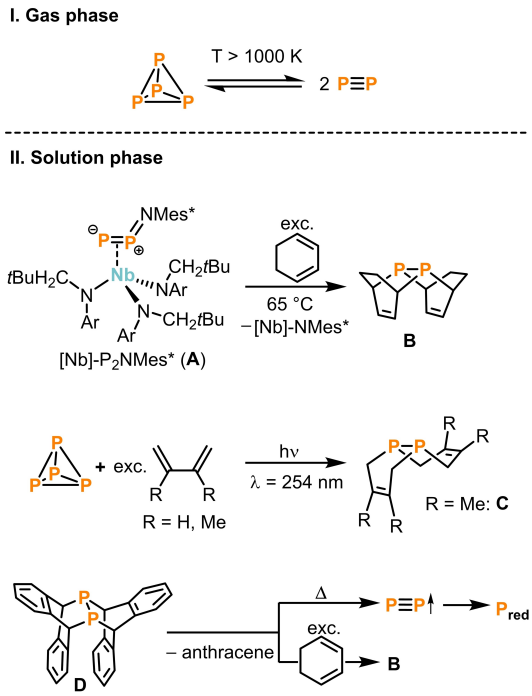

Figure 1. Examples of compounds capable of P_2 transfer; Mes* = 2,4,6-tri-*tert*-butylphenyl.[6,9,11]

[a] *Dr. G. Hierlmeier, Prof. Dr. R. Wolf*
Universität Regensburg, Institut für Anorganische Chemie
93040 Regensburg, Germany
E-mail: robert.wolf@ur.de
http://www.uni-regensburg.de/chemie-pharmazie/anorganische-chemie-wolf/index.html
[b] *Dr. G. Hierlmeier*
Princeton University, Department of Chemistry
Frick Laboratory 206, Princeton, NJ 08544, USA
E-mail: gh7941@princeton.edu

Supporting information for this article is available on the WWW under https://doi.org/10.1002/ejic.202101057

Research Article
doi.org/10.1002/ejic.202101057

units are released upon reaction of a phosphorus analogue of *p*-quinodimethane [(IPr=C)$_2$P$_4$] (IPr = 1,3-bis(2,6-di-*iso*-propylphenyl)imidazolin-2-ylidene) containing a planar P$_4$ ring with cyclohexadiene.[12] However, this reaction was not selective, affording both P$_4$ and the cycloaddition product **B**.

In 2018, we showed that the release of P$_2$ units is also viable using the dinuclear nickel butterfly complex [{(IMes)Ni(CO)}$_2$(μ^2,η^2:η^2-P$_2$)] (Figure 2, IMes = 1,3-bis(2,4,6-trimethylphenyl)imidazolin-2-ylidene) upon addition of carbon monoxide.[13] In the presence of 2,3-dimethylbutadiene (dmb), the formation of the diphosphine **C** was observed. In the absence of other reagents, however, P$_4$ was detected. The dimerisation of P$_2$-type units presumably takes place through a nickel-coordinated equivalent, since the dimerisation of free P$_2$ to P$_4$ is symmetry forbidden and therefore cannot take place under mild conditions.[6,14]

Since the use of toxic CO gas is a significant drawback of this method, we sought to develop alternatives for the release of P$_2$ from [{(IMes)Ni(CO)}$_2$(μ^2,η^2:η^2-P$_2$)]. Herein, we describe our efforts to use more convenient 2-electron donor ligands and heterocumulenes for the generation of diphosphorus and white phosphorus from [{(IMes)Ni(CO)}$_2$(μ^2,η^2:η^2-P$_2$)].

Results and Discussion

This study commenced with reactions of isonitriles with [{(IMes)Ni(CO)}$_2$(μ^2,η^2:η^2-P$_2$)]. Isonitriles were chosen because they are isoelectronic to carbon monoxide and often show similar reactivity. Unfortunately, the reaction of Cy–N≡C with [{(IMes)Ni(CO)}$_2$(μ^2,η^2:η^2-P$_2$)] afforded an intractable reaction mixture displaying multiple signals in the ^{31}P{^{1}H} NMR spectrum. We therefore turned our attention towards other two-electron donor ligands such as carbenes. Addition of excess amounts (8 equiv.) of the carbene 2,3,4,5-tetramethylimidazolin-2-ylidene (TMC, Figure 3) to an orange solution of [{(IMes)Ni(CO)}$_2$(μ^2,η^2:η^2-P$_2$)] in toluene resulted in a colour change to dark red. Analysis of the reaction mixture by ^{31}P{^{1}H} NMR spectroscopy revealed complete consumption of [{(IMes)Ni(CO)}$_2$(μ^2,η^2:η^2-P$_2$)] and formation of a single species characterised by a singlet resonance at 34.7 ppm. It is noteworthy that no P$_4$ was detected in the spectrum. Orange needles suitable for single crystal X-ray diffraction (SCXRD) were formed by slow diffusion of *n*-hexane into a benzene solution and revealed the formation of the dinuclear complex [{(TMC)$_2$Ni}$_2$(μ^2,η^2:η^2-P$_2$)] (**1**, Figure 3a).

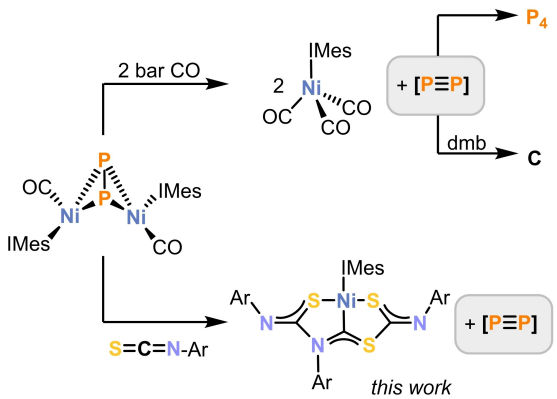

Figure 2. P$_4$ release via P$_2$-type intermediates from a nickel butterfly complex;[13] dmb = 2,3-dimethylbutadiene.

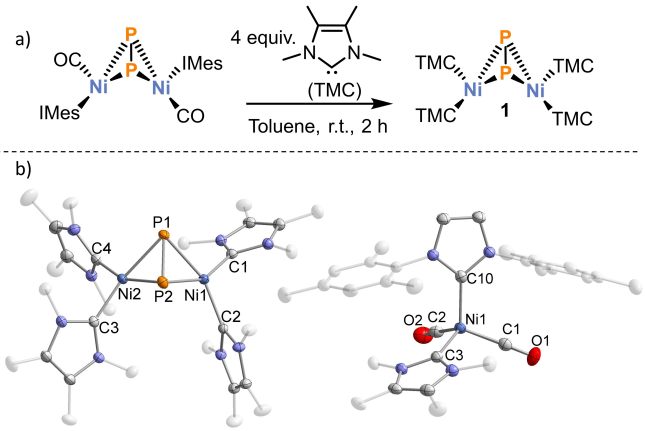

Figure 3. Synthesis of **1** (a) and molecular structures (b) of **1** and **2** in the solid state.[29] Thermal ellipsoids are set at the 50% probability level. Hydrogen atoms and solvent molecules (in case of **1**) are omitted for clarity. For **2**, 4 molecules with similar bond metric data are present in the asymmetric unit; the data for only one molecule are given below. Selected bond lengths [Å] and angles [°] for **1**: Ni1···Ni2 2.971(1), P1–P2 2.094(1), Ni1–P1 2.241(1), Ni1–P2 2.266(1), Ni1–C1 1.913(2), Ni1–C2 1.917(2), Ni2–P1 2.264(1), Ni2–P2 2.231(1), Ni2–C3 1.911(2), Ni2–C4 1.899(2), P1–Ni1–P2 55.3(1), P2–Ni2–P1 55.5(1), C1–Ni1–C2 106.5(1), C4–Ni2–C3 100.9(1), P2–P1–Ni2 61.4(1), P2–P1–Ni1 62.8(1), P1–P2–Ni2 63.0(1), Ni1–P1–Ni2 82.5(1), Ni2–P2–Ni1 82.6(1), Ni1/P1/P2 to Ni2/P1/P2 plane to plane fold angle 83.5(2); selected bond lengths [Å] and angles [°] for **2**: Ni1–C1 1.764(2), Ni1–C2 1.767(2), Ni1–C3 1.982(1), Ni1–C10 1.965(1), O1–C1 1.153(2), O2–C2 1.152(2), C10–Ni1–C3 108.0(1), C1–Ni1–C10 109.8(1), C1–Ni1–C3 107.4(1), C1–Ni1–C2 110.3(1), C2–Ni1–C10 109.0(1), C2–Ni1–C3 111.9(1).

Unexpectedly, **1** forms through ligand exchange of the carbonyl and IMes-ligands, retaining the Ni$_2$P$_2$ butterfly core. The P–P bond length of 2.094(1) Å compares well to the bond length in the starting material (2.076(2) Å).[13] Moreover, the Ni–C and Ni–P bond lengths (Ni–C 1.899(2)–1.917(2) Å and Ni–P 2.231(1)–2.266(1) Å, respectively) are in a comparable range to those observed for [{(IMes)(CO)Ni}$_2$(μ^2,η^2:η^2-P$_2$)]. **1** was isolated in a yield of 31% as a bright orange powder. The low yield is attributed to the presence of several other species in the ^{1}H NMR spectrum. One of these compounds was identified as the new NHC carbonyl complex [(IMes)(TMC)Ni(CO)$_2$] (**2**, Figure 3b) by SCXRD (see the SI for details).

The ^{1}H NMR spectrum of **1** in C$_6$D$_6$ solvent shows two signals at 1.97 and 3.58 ppm corresponding to the methyl groups of the carbene ligand. In the ^{31}P{^{1}H} NMR spectrum a singlet resonance at 34.7 ppm (*vide supra*) is observed. This resonance is in a comparable region for the related complex [{(*i*PrIm^{Me})$_2$Ni}$_2$(μ^2,η^2:η^2-P$_2$)] [*i*PrIm^{Me} = 1,3-di-*iso*-propylimidazolin-2-ylidene, δ (^{31}P{^{1}H}) = 70.7 ppm] reported by Radius and co-workers.[3] The UV/Vis absorption spectrum of **1** shows a broad band at 320 nm tailing into the green region of the spectrum (down to ca. 500 nm), which accounts for its orange colour.

Research Article
doi.org/10.1002/ejic.202101057

We next assessed the reactivity of [{(IMes)Ni(CO)}$_2$(μ^2,η^2:η^2-P_2)] toward heterocumulenes. While di-*iso*-propylcarbodiimide does not react with [{(IMes)Ni(CO)}$_2$(μ^2,η^2:η^2-P_2)] even at elevated temperatures, phenyl isothiocyanate reacts readily with [{(IMes)Ni(CO)}$_2$(μ^2,η^2:η^2-P_2)] to form a purple solution and P_4 as observed by $^{31}P\{^1H\}$ NMR spectroscopy (singlet at −519.1 ppm, see Figure S17 in the SI). Structural characterisation of deep purple crystals by SCXRD revealed the formation of the mononuclear complex [(IMes)Ni(η^3-(PhNCS)$_3$)] (**3a**, Figure 4a). The same compound **3a** can also be synthesised by reacting the vinyltrimethylsilane (vtms) nickel(0) complex [(IMes)Ni-(vtms)$_2$] with phenyl isothiocyanate. Using this procedure, the compound was isolated in 44% yield. In a similar vein, the substituted aryl isothiocyanates 2,6-dimethylphenyl isothiocyanate and 3,5-bis(trifluoromethyl)phenyl isothiocyanate react with [(IMes)Ni(vtms)$_2$] to form [(IMes)Ni(η^3-(ArNCS)$_3$)] (Ar = 2,6-Me_2-C_6H_3 (**3b**) and 3,5-$(CF_3)_2$-C_6H_3 (**3c**)] in 77% (**3b**) and 39% (**3c**) yield, respectively. While complex **3c** was also accessible starting from [{(IMes)Ni(CO)}$_2$(μ^2,η^2:η^2-P_2)] as a precursor, 2,6-$Me_2C_6H_3NCS$ only reacted very slowly with the P_2 complex at ambient temperature. Complexes **3a–c** contain pincer-type ligands formed through trimerisation of three ArNCS molecules in the coordination sphere of nickel.

The molecular structures of **3a–c** (Figure 4b) in the solid state show η^3-coordination of the nickel atom by two sulfur atoms and one carbon atom of the (ArNCS)$_3$ ligands, resulting in a classical pincer-type architecture. The structural data for all three complexes are similar; thus, only the data for **3a** will be discussed exemplarily in the following section. The coordination environment of the nickel atom is almost planar [sum of angles 360.1(1)°]. The two planar pentagons C2/N1/C1/Ni1/S2 and C1/S3/C3/S1/Ni1 are almost coplanar with a plane to plane twist angle of 3.1(1)° whereas the imidazole rings of the NHC are significantly displaced with respect to the planar (PhNCS)$_3$ scaffold with a plane to plane twist angle of 73.0(2)°. The Ni1–C1 bond length of 1.872(2) Å is shorter than the Ni1–C4 bond length (1.935(2) Å), which can be attributed to a partial double bond character of the Ni1–C1 bond.

NMR spectra of complexes **3a** and **3b** were recorded at 0 °C because the two complexes slowly decompose in solution at ambient temperature. Complex **3c** was more stable at ambient temperature, allowing for NMR characterisation at 300 K. The ^1H NMR spectra of all three complexes are in good agreement with their molecular structures determined by SCXRD. Three signals were observed for the methyl-groups of the IMes ligand, which indicates a hindered rotation around the N–C(Mes) bonds. Additional signals in the aromatic region (**3a–c**) and the aliphatic region (**3b**) arise from the aryl residues of the former isothiocyanates. In the $^{13}C\{^1H\}$ NMR spectrum the two carbene resonances of C4 and C1 were detected at 173.5 and 238.8 ppm (**3a**), 179.2 and 239.1 ppm (**3b**) and 168.6 and 241.9 ppm (**3c**), respectively. The assignment of these resonances was confirmed by ^1H-^{13}C-HMBC spectra. Complex **3c** gives rise to three resonances in the $^{19}F\{^1H\}$ NMR spectrum with chemical shifts of −62.6, −62.5 and −62.4 ppm in a 1:1:1 ratio, confirming the three different chemical environments of the CF_3 groups. The UV/Vis absorption spectra of compounds **3a–c** feature broad bands at 560–580 nm, which account for the purple colours in solution.

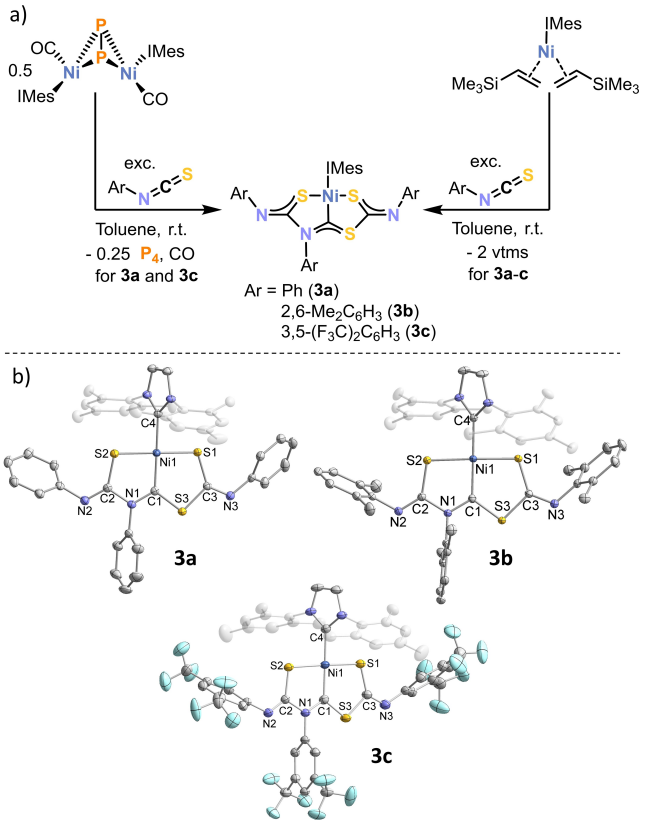

Figure 4. Synthesis (a) and molecular structures (b) of **3a**, **3b** and **3c** in the solid state.[29] Thermal ellipsoids are set at the 50% probability level. Hydrogen atoms, the second molecule in the asymmetric unit, solvent of crystallisation and positional disorder (for **3c**) are omitted for clarity. Selected bond lengths [Å] and angles [°] for **3a**: Ni1–C1 1.872(2), Ni1–C4 1.935(2), Ni1–S1 2.130(1), Ni1–S2 2.141(1), S3–C1 1.733(2), N1–C1 1.337(2), N1–C2 1.447(2), S2–C2 1.734(2), N2–C2 1.269(2), S3–C3 1.789(2), S1–C3 1.736(2), N3–C3 1.276(2), S1–Ni1–S2 175.7(1), C4–Ni1–S2 91.7(1), C4–Ni1–S1 88.7(1), C1–Ni1–S2 87.4(1), C1–Ni1–S1 92.2(1), C1–Ni1–C4 178.2(1), S3–C1–Ni1 124.2(1), N1–C1–Ni1 121.3(1), N1–C1–S3 114.4(1), NHC to Ni/S/C/N plane to plane twist angle 73.0(2). C2/N1/C1/Ni1/S2 to C1/S3/C3/S1/Ni1 plane to plane twist angle 3.1(1); for **3b**: Ni1–C1 1.871(1), Ni1–C4 1.936(1), Ni1–S1 2.139(1), Ni1–S2 2.167(1), S3–C1 1.726(1), N1–C1 1.335(2), N1–C2 1.438(2), S2–C2 1.733(1), N2–C2 1.272(2), S3–C3 1.784(1), S1–C3 1.729(1), N3–C3 1.277(2), S1–Ni1–S2 177.1(1), C4–Ni1–S2 92.0(1), C4–Ni1–S1 89.7(1), C1–Ni1–S2 86.8(1), C1–Ni1–S1 91.5(1), C1–Ni1–C4 174.1(1), S3–C1–Ni1 124.9(1), N1–C1–Ni1 121.6(1), N1–C1–S3 113.2(1), NHC to Ni/S/C/N plane to plane twist angle 57.2(1). C2/N1/C1/Ni1/S2 to C1/S3/C3/S1/Ni1 plane to plane twist angle 2.8(1). for **3c**: Ni1–C1 1.871(2), Ni1–C4 1.937(2), Ni1–S1 2.147(1), Ni1–S2 2.151(1), S3–C1 1.719(2), N1–C1 1.33(1), N1–C2 1.44(1), S2–C2 1.723(2), N2–C2 1.268(2), S3–C3 1.784(2), S1–C3 1.734(2), N3–C3 1.274(3), S1–Ni1–S2 178.4(1), C4–Ni1–S2 90.3(1), C4–Ni1–S1 90.4(1), C1–Ni1–S2 87.4(1), C1–Ni1–S1 91.7(1), C1–Ni1–C4 176.9(1), S3–C1–Ni1 125.0(1), N1–C1–Ni1 120.8(1), N1–C1–S3 114.0(1), NHC to Ni/S/C/N plane to plane twist angle 69.3(1). C2/N1/C1/Ni1/S2 to C1/S3/C3/S1/Ni1 plane to plane twist angle 0.7(1).

In order to gain further information on the electronic structure, density functional theory (DFT) calculations were performed on complex **3a**. The optimised structure (BP86-D3BJ/def2-TZVP level of theory) compares well with the experimental data. The HOMO of **3a** is mainly located at the two sulfur atoms coordinating to the Ni atom and the Ni atom

Research Article
doi.org/10.1002/ejic.202101057

itself (Figure 5 top). The LUMO is mostly located at the C1 atom with contributions from the adjacent nitrogen and carbon atoms. Inspection of the Mayer bond orders reveals a significant delocalisation of electrons along the N1–C1–S3 motif, as anticipated for a Fischer-type carbene (Figure 5 bottom). Moreover, the N2–C2–S2 and N3–C3–S1 moieties can be considered as delocalised heteroallylic systems. This is also in agreement

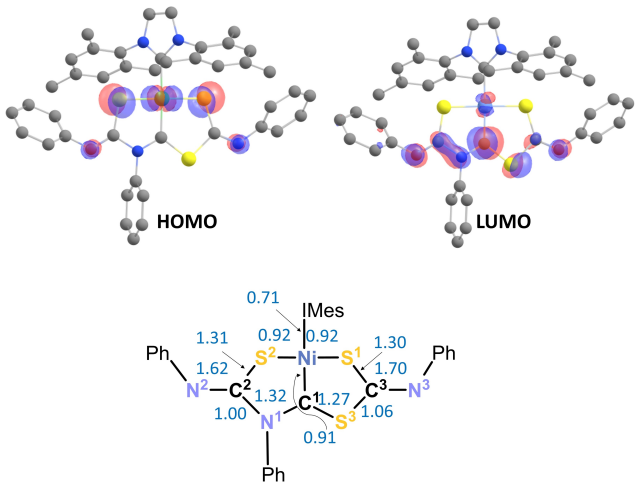

Figure 5. Highest occupied (HOMO) and lowest unoccupied (LUMO) orbitals of **3a** (isosurface value 0.05, top) and Mayer bond orders in **3a** (bottom).

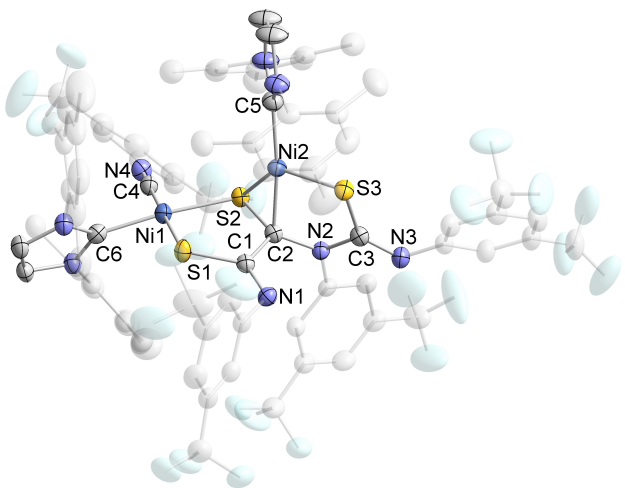

Figure 6. Molecular structure of **4** in the solid state.[29] Thermal ellipsoids are set at the 50% probability level. Hydrogen atoms, solvent of crystallisation (*n*-hexane) and positional disorder in the CF_3-groups are omitted for clarity. Selected bond lengths [Å] and angles [°]: Ni1–S1 2.161(1), Ni1–S2 2.211(1), Ni1–C6 1.922(2), Ni1–C4 1.812(3), Ni2–S2 2.204(1), Ni2–S3 2.146(1), Ni2–C2 1.922(2), Ni2–C5 1.917(3), S2–C2 1.769(2), S1–C1 1.759(2), S3–C3 1.758(2), N1–C1 1.281(3), N2–C2 1.437(3), N2–C3 1.397(3), N3–C3 1.288(3), N4–C4 1.157(3), C1–C2 1.478(3), S1–Ni1–S2 91.0(1), C6–Ni1–S2 173.7(1), C6–Ni1–S1 89.3(1), C4–Ni1–S2 87.0(1), C4–Ni1–S1 175.7(1), C4–Ni1–C6 92.1(1), S3–Ni2–S2 129.4(1), C2–Ni2–S2 50.1(1), C2–Ni2–S3 85.3(1), C5–Ni2–S2 123.4(1), C5–Ni2–S3 101.8(1), C5–Ni2–C2 172.7(1), N1–C1–S1 123.3(2), N1–C1–C2 119.0(2), C2–C1–S1 117.6(2), S2–C2–Ni2 73.2(1), N2–C2–Ni2 110.7(2), N2–C2–S2 118.6(2), N2–C2–C1 117.9(2), C1–C2–Ni2 109.2(2), C1–C2–S2 117.1(2), N2–C3–S3 113.6(2), N3–C3–S3 128.8(2), N3–C3–N2 117.6(2).

with the positive Löwdin atomic charges on the N2 and N3 atoms with values of 0.17 and 0.13, respectively.

In case of complex **3c**, the supernatant solution of the crystallisation contained crystals of an additional complex **4**, which was characterised by single crystal X-ray crystallography (Figure 6).

Complex **4** presumably forms upon prolonged storage of complex **3c** at ambient temperature. The molecular structure is composed of two nickel atoms, a trimer $(ArNCS)_3$ of three former aryl isothiocyanate molecules and an isonitrile ligand (ArNC), which is presumably formed from a fourth ArNCS molecule via loss of elemental sulfur. One of the nickel atoms (Ni1) is in a strictly square planar coordination environment [bond angles from 87.0(1)–92.1(1)°], while the coordination environment of the second nickel atom (Ni2) is more distorted [50.1(1)–123.4(1)°]. The N4–C4 bond length of 1.157(3) Å compares well to related nickel isonitrile complexes (e.g. $[Ni(NCPh)_4]$ 1.162(4) Å).[15] The new C1–C2 bond in **4** has a bond length of 1.478(3) Å which is in the range commonly observed for double bonds.[16] This is in line with the bond angles on the C1 atom [117.6(2) to 123.3(2)°], which indicate an sp^2-hybridised carbon atom in a trigonal planar environment. The C2 atom is tetracoordinate with a Ni1–C2 bond length of 1.922(2) Å. Unfortunately, compound **4** could not be isolated cleanly, preventing its full characterisation and further elucidation of its properties.

Notably, several reactions of organic isothiocyanates with transition metal complexes have been reported to date which result in insertions or oligomerisation reactions on the metal centre.[17,18] Only one system with a ligand comparable to the $(ArNCS)_3$ scaffold as in **3a–c** was described in the literature (complex **E**, Figure 7 left).[19] This complex contains rhodium in a similar coordination environment with two triphenylphosphine molecules, an additional chlorido ligand and an S–C–S pincer-type ligand obtained from ethoxycarbonyl isothiocyanate. However, in this case, a 1,3-shift of one of the substituents was observed, affording a two-coordinate N1-atom. Furthermore, it is noteworthy that a different, yet related P–C–S-type pincer complex **F** was reported recently by Gessner and co-workers.[20]

The successful reactions of (substituted) aryl isothiocyanates with $[(IMes)Ni(vtms)_2]$ inspired us to investigate similar reactions of cyclohexyl isothiocyanate CyNCS (Figure 8). In this case, a different product $[(IMes)Ni(\eta^3\text{-}(CyNCS)_2)]$ (**5**) can be isolated in 73% yield, which results from the dimerisation of CyNCS in the coordination sphere of nickel. A similar species $[(IPr)Ni(\eta^3\text{-}(PhNCS)_2)]$ was obtained in a recent study using [(IPr)Ni-

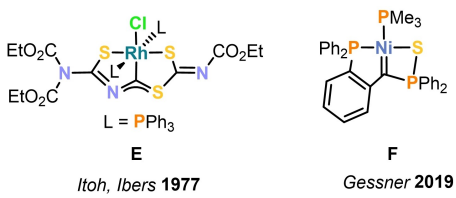

Figure 7. P–C–S– and S–C–S-type pincer ligands similar to those in **3a–c** described in literature.

Research Article
doi.org/10.1002/ejic.202101057

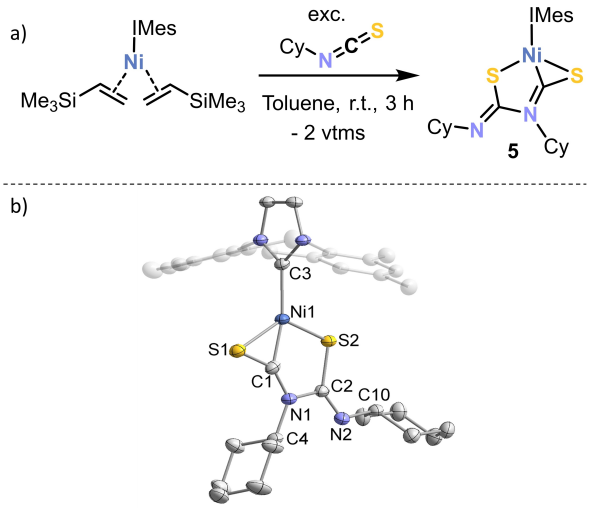

Figure 8. Synthesis (a) and molecular structure (b) of **5** in the solid state.[29] Thermal ellipsoids are set at the 50% probability level. Hydrogen are omitted for clarity. Selected bond lengths [Å] and angles [°]: Ni1–S1 2.282(1), Ni1–S2 2.150(1), Ni1–C1 1.755(3), Ni1–C3 1.933(3), S2–C2 1.772(3), S1–C1 1.646(3), N1–C1 1.319(3), N1–C2 1.437(3), N1–C4 1.488(3), N2–C2 1.266(4), S2–Ni1–S1 129.8(1), C1–Ni1–S2 83.9(1), C1–Ni1–S1 45.8(1), C1–Ni1–C3 166.5(1), C3–Ni1–S2 109.5(1), C3–Ni1–S1 120.6(1), C2–S2–Ni1 100.3(1), C1–S1–Ni1 49.8(1), N1–C2–S2 112.0(2) C1–N1–C2 111.9(2), N1–C1–Ni1 131.7(2), S2–Ni1–S1 129.8(1), C1–Ni1–S2 83.9(1), C1–Ni1–S1 45.8(1), C1–Ni1–C3 166.5(1), C3–Ni1–S2 109.5(1), C3–Ni1–S1 120.6(1), NHC to Ni/S/N plane to plane twist angle 90.1(1), Ni1/S1/C1 to Ni1/C1/N1/C2/S2 plane to plane twist angle 0.7(1).

(styrene)$_2$] instead of [(IMes)Ni(vtms)$_2$].[17] The molecular structures of **5** and [(IPr)Ni(η^3-(PhNCS)$_2$] are very similar, showing a planar coordination environment around the Ni atom and the imidazolylidene ligand in a perpendicular arrangements (for **5**, imidazole plane is twisted by 90.1(1)° with respect to the planar nickelacycle). The ^{1}H NMR spectrum of **5** dissolved in C_6D_6 corroborates the structure determined by X-ray crystallography. Two singlet resonances in a 1:2 ratio can be assigned to the methyl groups of the IMes ligand, suggesting free rotation around the N–C(Mes) bond. The cyclohexyl moieties give rise to multiplets in the region of 0.7–1.9 ppm and to triplets of triplets for the C^{4}H and C^{10}H protons of the cyclohexyl residues at chemical shifts of 4.23 and 4.50 ppm. In the ^{13}C{^{1}H} NMR spectrum, the carbene carbon atom features a resonance at 190.7 ppm, whereas the former heterocumulene carbon atoms C^1 and C^2 exhibit signals at 168.4 and 229.9 ppm. The UV/Vis absorption spectrum of **5** shows a broad band at 380 nm tailing up to 520 nm.

A possible explanation for the preference of CyNCS for dimerisaton is the increased steric bulk of cyclohexyl substituents in comparison to the planar aryl substituents. This explanation also covers the fact that reactions of PhNCS with less bulky IMes nickel complexes afford trimerised ligands like in **3a**, whereas using the bulkier carbene ligand IPr led to dimerisation to afford [(IPr)Ni(η^3-(PhNCS)$_2$].[17] Notably, however, electronic effects might also play a role for the preference for trimerisation over dimerisation.

Inspection of the coordination of the S–C–S pincer ligand in **3a–c** suggests that the nitrogen atoms in ArNCS are not essential for metal coordination. Therefore, it was hypothesised that isoelectronic carbon disulfide, CS_2, might undergo a similar reaction with [{(IMes)Ni(CO)}$_2$(μ^2,η^2:η^2-P$_2$)] or [(IMes)Ni(vtms)$_2$]. Indeed, addition of a CS_2 solution in THF to solutions of either of the complexes in benzene afforded a colour change from orange to red and precipitation of a red powder. ^{1}H NMR spectra of the red solid in THF-d$_8$ confirm the presence of one distinct IMes signal set, whereas the ^{31}P{^{1}H} NMR spectrum reveals formation of P_4 when [{(IMes)Ni(CO)}$_2$(μ^2,η^2:η^2-P$_2$)] is used as Ni-precursor. SCXRD analysis on crystals grown from fluorobenzene reveal the formation of the dinuclear complex [{(IMes)Ni(μ^2,η^1:η^2-CS$_2$)}$_2$] (**6**, Figure 9), which was isolated in 88% yield starting from [{(IMes)Ni(CO)}$_2$(μ^2,η^2:η^2-P$_2$)].

In the molecular structure of **6**, two sulfur atoms and a carbene-like carbon coordinate to planar nickel atoms. In contrast to **3a–c**, however, the complex is dinuclear and the CS_2-moieties are not directly connected, as was the case for the trimerised (PhNCS)$_3$ unit in **3a-c**. Each CS_2 moiety in **6** is η^2-coordinated via a C=S bond to one nickel atom and σ-bonded to the other nickel atom via the other sulfur atom. Similar to **3a–c**, the Ni1–C1 bond of 1.813(2) Å of the heteocumulene ligand is shorter than the Ni1–C2 bond (1.937(2) Å) formed by the NHC, the difference being more pronounced in case of **6** due to the small NiSC-ring.

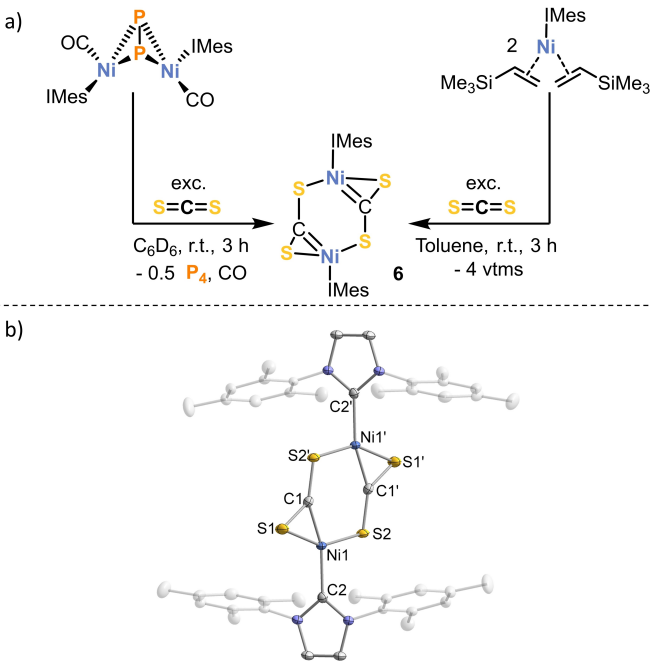

Figure 9. Synthesis (a) and molecular structure (b) of **6** in the solid state.[29] Thermal ellipsoids are set at the 50% probability level. Hydrogen atoms and solvent molecules are omitted for clarity. Selected bond lengths [Å] and angles [°]: Ni1–S1 2.181(1), Ni1–S2 2.158(1), Ni1–C1 1.813(2), Ni1–C2 1.937(2), S1–C1 1.664(2), S2–C1′ 1.662(1), S2–Ni1–S1 150.8(1), C1–Ni1–S1 48.1(1), C1–S1–Ni1 54.2 (1), S1–C1–Ni1 77.5(1), C1–S2–Ni1 110.0(1), C1–Ni1–S2 102.6(1), S2–C1–Ni1 147.2(1), C2–Ni1–S2 97.9(1), C2–Ni1–S1 111.2(1), NHC to Ni/S/C plane to plane twist angle 70.5(2).

Research Article
doi.org/10.1002/ejic.202101057

The ^{1}H NMR spectrum of **6** is in line with the molecular structure determined by SCXRD with a total of four singlet signals as expected for a C_{2v}-symmetric IMes ligand. The ^{13}C{^{1}H} NMR spectrum shows a strongly low-field-shifted carbene resonance for C1 at 285.6 ppm, which was assigned by ^{1}H-^{13}C-HMBC NMR spectroscopy. The NHC-carbene (C2) signal is observed at 189.2 ppm, similar to the shifts observed for **3a–c** (168.6–173.5 ppm). The UV/Vis absorption spectrum of **6** reveals an absorption band at 550 nm, which accounts for its red colour in solution.

A handful of compounds with structures closely related to **6** have been reported in the literature as deep red to purple solids, which were prepared by reacting CS_2 with nickel(0) N-heterocyclic carbene or phosphine ligands complexes.[17,18] A closely related example is the complex [{(*t*Bu$_2$Im)Ni(μ^2,η^1:η^2-CS$_2$)}$_2$] (*t*Bu$_2$Im = 1,3-di-*tert*-butylimidazolin-2-ylidene; Ni1–C1 1.810(2) Å, Ni1–C2 1.968(2) Å), which features similar structural and NMR parameters as compound **6**.[18]

Having firmly established that [{(IMes)Ni(CO)}$_2$(μ^2,η^2:η^2-P$_2$)] readily forms P_4 upon reaction with isothiocyanates and CS_2, we finally sought to trap the P_2 intermediate with 2,3-dimethylbutadiene. Unexpectedly, the desired diphosphine **C**, which was the major product when CO gas, could not be detected by ^{31}P NMR. Instead, the formation of several doublet resonances was observed (see Figures S15 and S16). Even though these signals hint towards the formation of nickel complexes of **C**, the isolation of cycloaddition products from [{(IMes)Ni(CO)}$_2$(μ^2,η^2:η^2-P$_2$)] unfortunately remains elusive.

Conclusion

Reactions of suitable two-electron donors with the Ni_2P_2 complex [{(IMes)Ni(CO)}$_2$(μ^2,η^2:η^2-P$_2$)] were investigated to study the utility of this complex as a source of P_2 units. While addition of tetramethylcarbene to [{(IMes)Ni(CO)}$_2$(μ^2,η^2:η^2-P$_2$)] only resulted in a ligand exchange reaction to form the symmetric complex **1**, heterocumulenes replaced the P_2 ligand effectively to afford P_4 and the new complexes **3a–c**, **4**, **5** and **6** which contain S–C–S pincer-type carbene ligands with planar coordination geometries around the nickel atom and an NHC ancillary ligand. Aryl-substituted isocyanates ArNCS undergo a trimerisation within the coordination sphere of nickel to form unusual (ArNCS)$_3$ scaffolds observed in the structures of **3a–c**, while CS_2 coordinates in an η^2-fashion and forms a dinuclear complex. The same complexes **3**–**6** can be prepared by the simple reaction of the heterocumulene with the readily available Ni(0) complex [(IMes)Ni(vtms)$_2$].

While the P_2 ligand in [{(IMes)Ni(CO)}$_2$(μ^2,η^2:η^2-P$_2$)] appears to be easily liberated, trapping reactions with 2,3-dimethylbutadiene turned out to be unsuccessful. Although the reasons for this reactivity are currently not entirely unclear, it is tempting to speculate that the cycloaddition products coordinate to nickel fragments to form several unidentified complexes. Furthermore, it is possible that the P_2 type fragments undergo unselective reactions with the heterocumulenes themselves. Further investigations into the release of P_2 from Ni_2P_2 complexes and the subsequent trapping of the P_2 moiety therefore appear to be worthwhile.

Experimental Section

General Synthetic Methods

All reactions and product manipulations were carried out in flame-dried glassware under an inert atmosphere of argon using standard Schlenk-line or glovebox techniques (maintained at <0.1 ppm H_2O and <0.1 ppm O_2). Tetramethylcarbene (TMC)[21], [{(IMes)Ni(CO)}$_2$(μ^2,η^2:η^2-P$_2$)][13] and [(IMes)Ni(vtms)$_2$][22] were prepared according to procedures previously reported in the chemical literature. All other chemicals were purchased from commercial suppliers and used without further purification.

Solvents were dried and degassed with an MBraun SPS800 solvent purification system. Fluorobenzene was dried over sodium and distilled. All dry solvents except *n*-hexane were stored under argon over activated 3 Å molecular sieves in gas-tight ampules. *n*-Hexane was instead stored over a potassium mirror.

General Analytical Techniques

NMR spectra were recorded on Bruker Avance 300 or 400 spectrometers at 300 K unless otherwise noted and internally referenced to residual solvent resonances (^{1}H NMR: THF-d$_8$: 1.72 ppm, C_6D_6: 7.16 ppm, toluene-d$_8$: 2.08 ppm; ^{13}C{^{1}H} NMR: THF-d$_8$: 25.31 ppm, C_6D_6: 128.06 ppm, toluene-d$_8$: 20.43 ppm). Chemical shifts δ are given in ppm referring to external standards of tetramethylsilane (^{1}H, ^{13}C{^{1}H}), 85% phosphoric acid (^{31}P and ^{31}P{^{1}H}). ^{1}H and ^{13}C NMR signals were assigned based on 2D NMR spectra (^{1}H,^{1}H-COSY, ^{1}H,^{13}C-HSQC, ^{1}H,^{13}C-HMQC).

UV/Vis absorption spectra were recorded on an Ocean Optics Flame Spectrometer. Elemental analysis was performed by the Central Analytical Services department of the University of Regensburg.

Single-crystal X-ray diffraction data were recorded on a Rigaku Oxford Diffraction SuperNova Atlas or a XtaLAB Synergy R (DW system, Hypix-Arc 150) device with Cu-K_α radiation ($\lambda = 1.54184$ Å). Crystals were selected under mineral oil, mounted on micromount loops and quench-cooled using an Oxford Cryosystems open flow N_2 cooling device. Either semi-empirical multi-scan absorption corrections[23] or analytical ones[24] were applied to the data. The structures were solved with SHELXT[25] solution program using dual methods and by using Olex2 as the graphical interface.[26] The models were refined with ShelXL[27] using full matrix least squares minimisation on F^2.[28] The hydrogen atoms were located in idealised positions and refined isotropically with a riding model.

Synthesis of Compounds

[{(TMC)$_2$Ni}$_2$(μ^2,η^2:η^2-P$_2$)] (1)

To a solution of [{(IMes)Ni(CO)}$_2$(μ^2,η^2:η^2-P$_2$)]·(0.5 *n*-hexane) (110.0 mg, 0.124 mmol, 1.0 equiv.) in toluene (6 mL) was added TMC (61.6 mg, 0.50 mmol, 4.0 equiv.). Upon stirring at ambient temperature for 2 hours, a colour change from deep orange to deep red was observed. Subsequently, the solvent was removed, and the dark red residue was dried *in vacuo*. The residue was washed with *n*-hexane (5 mL) and benzene (5 mL) and the resulting bright orange solid was dried *in vacuo* to afford pure [{(TMC)$_2$Ni}$_2$(μ^2,η^2:η^2-P$_2$)]. Crystals of [{(TMC)$_2$Ni}$_2$(μ^2,η^2:η^2-P$_2$)] (**1**) suitable for X-ray crystallography were grown by slow diffusion of *n*-

hexane into a saturated solution of **1** in benzene. In addition, X-ray quality crystals of [(IMes)(TMC)Ni(CO)$_2$] (**2**) were obtained from the benzene washing solution after storage for 2 months at ambient temperature.

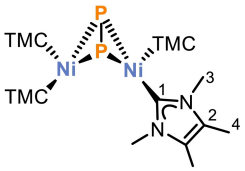

$C_{28}H_{48}N_8Ni_2P_2$, MW = 676.08 g/mol, yield: 26 mg (31 %). ^{1}H NMR (400 MHz, 300 K, THF-d$_8$) δ = 1.97 (s, 24H, C^{4}H), 3.58 (s, 24H, C^{3}H) ppm. ^{13}C{^{1}H} NMR (100 MHz, 300 K, THF-d$_8$) δ = 9.2 (s, C^4), 34.8 (s, C^3), 122.7 (s, C^2), 203.5 (br s, C^1) ppm. ^{31}P{^{1}H} (162 MHz, 300 K, THF-d$_8$) δ = 34.7 (s) ppm. Elemental Analysis calcd. C 49.74, H 7.16, N 16.57; found C 49.46, H 7.21, N 15.28. UV/Vis (THF): λ_{max} (nm, ε_{max}/L mol^{-1} cm^{-1}) 320 (21 000).

[(IMes)Ni(η^3-(PhNCS)$_3$)] (3 a)

To a solution of [(IMes)Ni(vtms)$_2$] (100.0 mg, 0.177 mmol, 1.0 equiv.) in toluene (5 mL) was added phenyl isothiocyanate (0.1 mL, 113 mg, 0.84 mmol, 4.7 equiv.). The colour of the reaction mixture changed from yellow over burgundy to deep purple while stirring at ambient temperature for 1.5 h. Subsequently, the solvent was removed, and the dark residue was dried *in vacuo*. The residue was washed with *n*-hexane (20 mL), extracted in toluene (3 mL) and layered with *n*-hexane (20 mL). Storage at −30 °C for 3 days afforded microcrystalline [(IMes)Ni(η^3-PhNCS)$_3$] which was isolated by decanting the supernatant and dried *in vacuo*. Crystals of [(IMes)Ni(η^3-PhNCS)$_3$] (**3 a**) suitable for X-ray crystallography were grown by slow diffusion of *n*-hexane into a saturated solution of **3 a** in toluene.

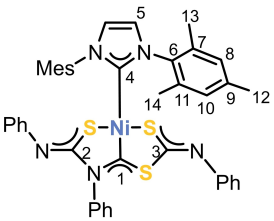

$C_{42}H_{39}N_5NiS_3$, MW = 768.68 g/mol, yield: 60 mg (44 %).^{1}H NMR (400 MHz, 273 K, toluene-d$_8$) δ = 2.03 (s, 6H, C^{12}H), 2.16 (s, 6H, C^{13}H), 2.19 (s, 6H, C^{14}H), 5.96–5.98 (m, 2H, H^{Ph}), 5.99 (s, 2H, C^{5}H), 6.69–6.73 (m, 4H, H^{Ph}), 6.75 (s, 2H, C^{10}H), 6.76 (s, 2H, C^{8}H), 7.22–7.34 (m, 9H, H^{Ph}) ppm. ^{13}C{^{1}H} NMR (100 MHz, 273 K, toluene-d$_8$) δ = 19.17 (s, C^{13}), 19.22 (s, C^{14}), 21.0 (s, C^{12}, overlapping with toluene signal), 122.2 (s, C^{Ar}), 122.6 (s, C^{Ar}), 123.6 (s, C^{Ar}), 123.7 (s, C^{Ar}), 124.5 (s, C^5), 126.8 (s, C^{Ar}), 128.47 (s, C^{Ar}, overlapping with toluene signal), 128.5 (s, C^{Ar}, overlapping with toluene signal), 129.5 (s, C^{10}), 129.6 (s, C^8), 135.7 (s, C^6), 135.9 (s, C^{11}), 136.0 (s, C^7), 139.2 (s, C^{Ar}), 143.1 (s, C^{Ar}), 149.6 (s, C^{Ar}), 151.5 (s, C^{Ar}), 169.8 (s, C$^{2/3}$), 173.5 (s, C^4), 180.4 (s, C$^{2/3}$), 238.8 (s, C^1) ppm. 11 signals in the aromatic region (labelled with C^{Ar}) could not be assigned to specific carbon atoms. The number of signals is smaller than expected in case of free rotation around C–N(Ph) and hindered rotation around C–N(Mes) (18 signals expected, 5 signals (assigned to the Mes-group) were assigned by 2D NMR spectroscopy). This could be explained by similar chemical environments of the phenyl groups and overlapping signals. Elemental Analysis calcd. C 65.63, H 5.11, N 9.11, S 12.51; found C 65.66, H 5.15, N 8.70, S 11.31. UV/Vis (THF): λ_{max} (nm, ε_{max}/L mol^{-1} cm^{-1}) 280 (31 000), 340 (12 500sh), 580 (3200). [(IMes)Ni(η^3-(PhNCS)$_3$)] (**3 a**) can also be prepared by an analogous procedure to the one described using 0.5 equiv. [{(IMes)Ni(CO)}$_2$(μ^2,η^2:η^2-P$_2$)] (30.0 mg, 0.034 mmol). Yield: 17 mg (65 %). Spectroscopic and analytical data of the isolated compound were identical to those given above.

[(IMes)Ni(η^3-(2,6-Me$_2$C$_6$H$_3$NCS)$_3$)] (3 b)

To a solution of [(IMes)Ni(vtms)$_2$] (30.0 mg, 0.053 mmol, 1.0 equiv.) in toluene (2 mL) was added an excess amount of 2,6-dimethylphenyl isothiocyanate (0.1 mL, 109 mg, 0.67 mmol, 13.5 equiv.). The colour of the reaction mixture changed from yellow over burgundy to deep purple while stirring at ambient temperature for 1.5 h. Subsequently, the solvent was removed and the dark residue was dried *in vacuo*. The residue was washed with *n*-hexane (5 mL), extracted in benzene (1 mL) and layered with *n*-hexane (5 mL). Storage at ambient temperature overnight afforded crystals of [(IMes)Ni(η^3-(2,6-Me$_2$C$_6$H$_3$NCS)$_3$)] (**3 b**) which were isolated by decanting the supernatant. The crystals were dried *in vacuo*. Crystals of **3 b** suitable for X-ray crystallography were grown by slow diffusion of *n*-hexane into a saturated solution of **3 b** in benzene.

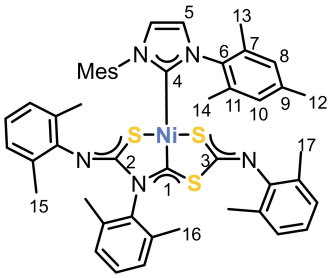

$C_{48}H_{51}N_5NiS_3$, MW = 852.84 g/mol, yield: 35 mg (77 %), ^{1}H NMR (400 MHz, 273 K, toluene-d$_8$) δ = 1.86 (s, 6H, CH$_3$), 1.97 (s, 6H, CH$_3$), 1.99 (s, 6H, CH$_3$), 2.11 (s, 6H, CH$_3$), 2.16 (s, 6H, CH$_3$), 2.26 (s, 6H, CH$_3$), 5.86 (s, 2H, C^{5}H), 6.64–6.72 (m, 4H, C^{Ar}H), 6.75 (s, 2H, C^{Ar}H), 6.83 (t, $^3J_{HH}$ = 7.6 Hz, C^{Ar}H), 6.93 (dd, 1H, *J* = 6.8, 8.0 Hz, C^{Ar}H), 6.99 (br s, 1H, overlapping with solvent signal, C^{Ar}H), 7.02–7.04 (m, 2H, overlapping with solvent signal, C^{Ar}H), 7.08–7.14 (m, 2H, overlapping with solvent signal, C^{Ar}H) ppm. ^{13}C{^{1}H} NMR (100 MHz, 273 K, toluene-d$_8$) δ = 17.4 (s, C$^{15/16/17}$), 18.4 (s, C$^{15/16/17}$), 19.0 (s, C$^{15/16/17}$), 19.1 (s, C$^{13/14}$), 19.2 (s, C$^{13/14}$), 21.1 (s, C^{12}), 123.0 (s, C^{Ar}), 124.3 (s, C^5), 127.2 (s, C^{Ar}), 127.37 (s, C^{Ar}), 127.43 (s, C^{Ar}), 129.37 (s, C^{Ar}), 129.41 (s, C^{Ar}), 134.2 (s, C^{Ar}), 135.5 (s, C^{Ar}), 135.6 (s, C^{Ar}), 135.88 (s, C^{Ar}), 135.90 (s, C^{Ar}), 138.6 (s, C^{Ar}), 142.3 (s, C^{Ar}), 147.7 (s, C^{Ar}), 150.6 (s, C^{Ar}), 167.9 (s, C$^{2/3}$), 173.4 (s, C^4), 179.2 (s, C$^{2/3}$), 239.1 (s, C^1) ppm. 15 signals in the aromatic region (labelled with C^{Ar}) in the ^{13}C{^{1}H} NMR spectrum could not be assigned to specific carbon atoms. The number of signals is smaller than expected in case of free rotation around C–N(Dmp) and hindered rotation around C–N(Mes) (18 signals expected). This could be explained by similar chemical environments of the Dmp-groups and overlapping signals. Elemental Analysis calcd. C 67.60, H 6.03, N 8.21, S 11.28; found C 68.43, H 6.08, N 8.12, S 11.60. UV/Vis (THF): λ_{max} (nm, ε_{max}/L mol^{-1} cm^{-1}) 280 (19 000), 380 (3000sh), 560 (1500).

[(IMes)Ni(η^3-(3,5-(CF$_3$)$_2$C$_6$H$_3$NCS)$_3$)] (3 c)

To a solution of [(IMes)Ni(vtms)$_2$] (50.0 mg, 0.089 mmol, 1.0 equiv.) in toluene (2 mL) was added an excess amount of 3,5-bis(trifluoromethyl)phenyl isothiocyanate (0.1 mL, 149 mg, 0.55 mmol, 10.4 equiv.). The colour of the reaction mixture immediately changed from yellow over burgundy to deep purple while stirring at ambient temperature for one hour. Subsequently, the solvent was removed and the dark residue was dried *in vacuo*. The residue was extracted with *n*-hexane (3 mL). Storage at

Research Article
doi.org/10.1002/ejic.202101057

ambient temperature overnight afforded crystals of [(IMes)Ni(η^3-(3,5-$(CF_3)_2C_6H_3NCS)_3$)] (**3 c**) suitable for X-ray crystallography. These crystals were isolated by decanting the supernatant and dried *in vacuo*. Storage of the supernatant solution at ambient temperature for 5 days afforded brown crystals of **4** suitable for X-ray crystallography along with crystals of **3 c**.

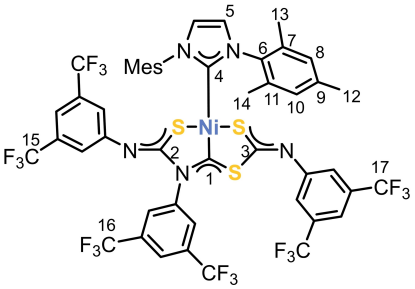

$C_{48}H_{33}F_{18}N_5NiS_3 \cdot 0.45$(*n*-hexane), MW = 1176.67 (+38.78) g/mol, yield: 42 mg (39 %). ^{1}H NMR (400 MHz, 300 K, C_6D_6) δ = 1.93 (s, 6H, C^{12}H), 2.12 (s, 6H, $C^{13/14}$H), 2.13 (s, 6H, $C^{13/14}$H), 5.92 (s, 2H, C^5H), 6.42 (s, 2H, C^{ArF}ortho-H), 6.80 (s, 4H, $C^{8/10}$H), 7.45 (s, 1H, C^{ArF}para-H), 7.51 (s, 1H, C^{ArF}para-H), 7.58 (s, 1H, C^{ArF}para-H), 7.64 (s, 2H, C^{ArF}ortho-H), 7.65 (s, 2H, C^{ArF}ortho-H) ppm. ^{13}C{^{1}H} NMR (100 MHz, 300 K, C_6D_6) δ = 18.7 (s, $C^{13\&14}$), 20.8 (s, C^{12}), 117.6 (m, C^{ArF}para), 117.8 (m, C^{ArF}para), 120.0 (m, C^{Ar}), 121.3 (s, C^{Ar}), 122.5 (m, C^{ArF}ortho), 122.7 (m, C^{ArF}ortho), 123.6 (m, C^{ArF}para), 124.1 (s, C^{Ar}), 125.4 (s, C^5), 125.7 (m, C^{Ar}), 129.95 (s, $C^{8/10}$), 129.99 (s, $C^{8/10}$), 132.3 (q, $^1J_{CF}$ = 33.1 Hz, $C^{15/16/17}$), 132.4 (q, $^1J_{CF}$ = 33.0 Hz, $C^{15/16/17}$), 133.2 (q, $^1J_{CF}$ = 34.5 Hz, $C^{15/16/17}$), 135.4 (s, C^{Ar}), 135.5 (s, C^{Ar}), 135.7 (s, C^{Ar}), 140.3 (s, C^{Ar}), 143.1 (s, C^{Ar}), 150.0 (s, C^{Ar}), 151.7 (s, C^{Ar}), 168.6 (s, C^4), 172.7 (s, $C^{2/3}$), 182.8 (s, $C^{2/3}$), 241.9 (s, C^1) ppm. 11 signals in the aromatic region (labelled with C^{Ar}) in the ^{13}C{^{1}H} NMR spectrum could not be assigned to specific carbon atoms. Nevertheless, the number of observed signals equals the number of inequivalent carbon atoms (18 signals) expected for free rotation around N–C(Ar^F) and hindered rotation around N–C(Mes), 7 of these signals were assigned by 2D NMR spectroscopy. ^{19}F{^{1}H} NMR (377 MHz, 300 K, C_6D_6) δ = −62.6 (s, 6F, $C^{15/16/17}$F), −62.5 (s, 6F, $C^{15/16/17}$F), −62.4 (s, 6F, $C^{15/16/17}$F) ppm. Elemental Analysis [for **3 c**·0.45(*n*-hexane), MW = 1215.45 g/mol] calcd. C 50.10, H 3.26, N 5.76, S 7.91; found C 49.76, H 3.13, N 5.80, S 7.35. UV/Vis (THF): λ_{max} (nm, ε_{max}/L mol^{-1} cm^{-1}) 280 (48 000), 330 (30 000sh), 400 (7000sh), 580 (4000). [(IMes)Ni(η^3-3,5-$(F_3C)_2C_6H_3NCS)_3$)] (**3 c**) can also be prepared by an analogous procedure to the one described using 0.5 equiv. [{(IMes)Ni(CO)}$_2$(μ^2,η^2:η^2-P_2)]. (30.0 mg, 0.034 mmol). Yield: 24 mg (29 %). Spectroscopic and analytical data of the isolated compound were identical to those given above.

[(IMes)Ni(η^2-$(CyNCS)_2$)] (5)

To a solution of [(IMes)Ni(vtms)$_2$] (20.0 mg, 0.036 mmol, 1.0 equiv.) in toluene (5 mL) was added an excess amount of cyclohexyl isothiocyanate (0.1 mL, 99.6 mg, 0.71 mmol, 19.6 equiv.) at −30 °C. After stirring at ambient temperature for 5 minutes a colour change from yellow to orange was observed. The reaction mixture was stirred for 2 hours in total. Subsequently, the solvent was removed and the residue was dried *in vacuo*. The residue was extracted with *n*-hexane (5 mL) and stored at ambient temperature overnight to afford orange crystals of [(IMes)Ni(η^2-$(CyNCS)_2$)] (**5**) suitable for single crystal X-ray diffraction. The crystals were isolated by decanting the supernatant and dried *in vacuo*.

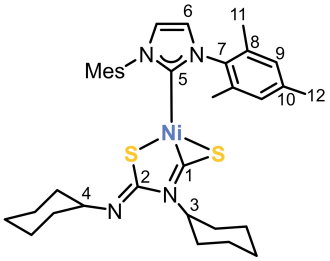

$C_{35}H_{46}N_4NiS_2 \cdot 0.2$(*n*-hexane), MW = 645.59 (+ 17.24) g/mol, yield: 17 mg (71 %). ^{1}H NMR (400 MHz, 300 K, C_6D_6) δ = 0.60–1.84 (m, 20H, Cy–H), 2.03 (s, 6H, C^{12}H), 2.11 (m, 2H, Cy–H), 2.22 (s, 12H, C^{11}H), 4.23 (tt, $^3J_{HH}$ = 9.8 Hz, 4.3 Hz, $C^{3/4}$H), 4.50 (tt, 12.2 Hz, 3.6 Hz, $C^{3/4}$H), 6.21 (s, 2H, C^6H), 6.75 (s, 4H, C^9H) ppm. ^{13}C{^{1}H} NMR (100 MHz, 300 K, C_6D_6) δ = 18.2 (s, C^{11}), 21.09 (s, C^{12}), 23.1 (s, C^{Cy}), 23.2 (s, C^{Cy}), 25.0 (s, C^{Cy}), 25.3 (s, C^{Cy}), 25.5 (s, C^{Cy}), 25.6 (s, C^{Cy}), 26.7 (s, C^{Cy}), 30.3 (s, C^{Cy}), 33.0 (s, C^{Cy}), 34.1 (s, C^{Cy}), 58.0 (s, $C^{3/4}$), 58.7 (s, $C^{3/4}$), 122.4 (s, C^6), 129.5 (s, C^9), 135.6 (s, C^7), 136.8 (s, C^7), 138.8 (s, C^{10}), 168.4 (s, $C^{1/2}$), 190.7 (s, C^5), 229.9 (s, $C^{1/2}$) ppm. Elemental Analysis [for **5**·0.2(*n*-hexane), MW = 662.83 g/mol] calcd. C 65.60, H 7.42, N 8.45, S 9.67; found C 65.75, H 7.28, N 8.48, S 10.00. UV/Vis (THF): λ_{max} (nm, ε_{max}/L mol^{-1} cm^{-1}) 270 (28 000), 380 (4 300, tailing to 520 nm).

[{(IMes)Ni(μ^2,η^1:η^2-CS_2)}$_2$] (6)

To a suspension of [{(IMes)Ni(CO)}$_2$(μ^2,η^2:η^2-P_2)]·(0.5 *n*-hexane) (40.0 mg, 0.045 mmol, 1.0 equiv.) in *n*-hexane (5 mL) was added an excess amount of CS_2 (0.1 mL, 5 mol L^{-1} in THF, 0.5 mmol, 11.0 equiv.). While stirring at ambient temperature for 30 minutes a colour change from yellow to deep red and the formation of a red precipitate was observed. The reaction mixture was filtered, and the remaining red powder was dried *in vacuo*, resulting in analytically pure [{(IMes)Ni(μ^2,η^1:η^2-CS_2)}$_2$] (**5**). Crystals of [{(IMes)Ni(μ^2,η^1:η^2-CS_2)}$_2$] (6) suitable for X-ray crystallography were grown by slow diffusion of *n*-hexane into a saturated solution of **6** in fluorobenzene.

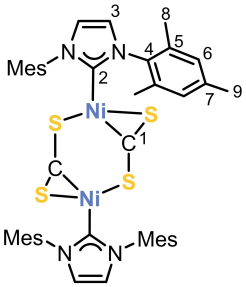

$C_{44}H_{48}N_4Ni_2S_4$, MW = 878.52 g/mol, yield: 35 mg (88 %).^{1}H NMR (400 MHz, 300 K, C_6D_6) δ = 1.99 (s, 24H, C^8H), 2.01 (s, 12H, C^9H), 6.04 (s, 4H, C^3H), 6.42 (s, 8H, C^6H) ppm. ^{13}C{^{1}H} NMR (100 MHz, 300 K, C_6D_6) δ = 18.2 (s, C^8), 21.2 (s, C^9), 122.7 (s, C^3), 129.4 (s, C^6), 135.1 (s, C^4), 136.4 (s, C^5), 138.0 (s, C^7), 189.2 (s, C^2), 285.6 (s, C^1) ppm. Elemental Analysis calcd. C 60.16, H 5.51, N 6.38; found C 60.11, H 5.57, N 6.83. UV/Vis (THF): λ_{max} (nm, ε_{max}/L mol^{-1} cm^{-1}) 380 (11 500), 550 (7000).

[{(IMes)Ni(μ^2,η^1:η^2-CS_2)}$_2$] (**5**) can also be prepared by an analogous procedure to the one described using 2.0 equiv. [(IMes)Ni(vtms)$_2$] (50.0 mg, 0.089 mmol). Yield: 35 mg (90 %). NMR spectroscopic data of the isolated compound were identical to those given above.

Acknowledgements

Financial support by the Fonds der Chemischen Industrie (Kekulé fellowship for G.H.) and the European Research Council (ERC CoG 772299) is gratefully acknowledged. We thank Maria Uttendorfer for assistance with elemental analyses. Open Access funding enabled and organized by Projekt DEAL.

Conflict of Interest

The authors declare no conflict of interest.

Data Availability Statement

The data that support the findings of this study are available in the supplementary material of this article.

Keywords: Heterocumulenes · Nickel · Oligomerisation · Phosphorus · Pincer ligands

[1] P. Jutzi, *Angew. Chem. Int. Ed. Engl.* **1975**, *14*, 232–245.
[2] A. Sekiguchi, R. Kinjo, M. Ichinohe, *Science* **2004**, *305*, 1755–1757.
[3] B. Zarzycki, T. Zell, D. Schmidt, U. Radius, *Eur. J. Inorg. Chem.* **2013**, 2051–2058.
[4] a) H. Schäfer, D. Binder, D. Fenske, *Angew. Chem. Int. Ed. Engl.* **1985**, *24*, 522–524; b) J. E. Davies, M. C. Klunduk, P. R. Raithby, G. P. Shields, P. K. Tompkin, *J. Chem. Soc. Dalton Trans.* **1997**, 715–719; c) L. Y. Goh, C. K. Chu, R. C. S. Wong, *J. Chem. Soc. Dalton Trans.* **1989**; d) O. J. Scherer, H. Sitzmann, G. Wolmershäuser, *J. Organomet. Chem.* **1984**, C9-C12; e) C. F. Campana, A. Vizi-Orosz, G. Palyi, L. Marko, L. F. Dahl, *Inorg. Chem.* **1979**, *11*, 3054–3059; f) M. Demange, X.-F. Le Goff, P. Le Floch, N. Mézailles, *Chem. Eur. J.* **2010**, *16*, 12064–12068; g) J. S. Figueroa, C. C. Cummins, *J. Am. Chem. Soc.* **2003**, *125*, 4020–4021.
[5] J. Sun, H. Verplancke, J. I. Schweizer, M. Diefenbach, C. Würtele, M. Otte, I. Tkach, C. Herwig, C. Limberg, S. Demeshko, M. C. Holthausen, S. Schneider, *Chem* **2021**, *70*, 2140.
[6] H. Bock, H. Mueller, *Inorg. Chem.* **1984**, *23*, 4365–4368.
[7] O. J. Scherer, *Angew. Chem. Int. Ed.* **2000**, *39, 1029*, 1029–1030.
[8] N. A. Piro, J. S. Figueroa, J. T. McKellar, C. C. Cummins, *Science* **2006**, *313*, 1276–1279.
[9] D. Tofan, C. C. Cummins, *Angew. Chem. Int. Ed.* **2010**, *49*, 7516–7518; *Angew. Chem.* **2010**, *122*, 7678–7680.
[10] L.-P. Wang, D. Tofan, J. Chen, T. van Voorhis, C. C. Cummins, *RSC Adv.* **2013**, *3*, 23166.
[11] A. Velian, M. Nava, M. Temprado, Y. Zhou, R. W. Field, C. C. Cummins, *J. Am. Chem. Soc.* **2014**, *136*, 13586–13589.
[12] D. Rottschäfer, B. Neumann, H.-G. Stammler, R. Kishi, M. Nakano, R. S. Ghadwal, *Chem. Eur. J.* **2019**, *25*, 3244–3247.
[13] G. Hierlmeier, A. Hinz, R. Wolf, J. M. Goicoechea, *Angew. Chem. Int. Ed.* **2018**, *57*, 431–436; *Angew. Chem.* **2018**, *130*, 439–444.
[14] H. W. Melville, S. C. Gray, *Trans. Faraday Soc.* **1936**, *32*, 271.
[15] F. E. Hahn, M. Münder, R. Fröhlich, *Z. Naturforsch. B* **2004**, *59*, 850–854.
[16] a) P. Pyykkö, *J. Phys. Chem. A* **2015**, *119*, 2326–2337; b) B. Cordero, V. Gómez, A. E. Platero-Prats, M. Revés, J. Echeverría, E. Cremades, F. Barragán, S. Alvarez, *Dalton Trans.* **2008**, 2832–2838; c) P. Pyykkö, M. Atsumi, *Chem. Eur. J.* **2009**, *15*, 186–197.
[17] S. Pelties, R. Wolf, *Organometallics* **2016**, *35*, 2722–2727.
[18] a) C. Bianchini, D. Masi, C. Mealli, A. Meli, *J. Organomet. Chem.* **1983**, *247*, C29–C31; b) P. Jernakoffm, N. J. Cooper, *J. Am. Chem. Soc.* **1989**, *111*, 7424–7430; c) Q. Shen, H. Li, C. Yao, Y. Yao, L. Zhang, K. Yu, *Organometallics* **2001**, *20*, 3070–3073; d) Y.-J. Kim, J.-T. Han, S. Kang, W. S. Han, S. W. Lee, *Dalton Trans.* **2003**, 3357–3364; e) C. Wycliff, A. G. Samuelson, M. Nethaji, *Inorg. Chem.* **1996**, *35*, 5427–5434; f) W. Mei, L. Shiwei, B. Meizhi, G. Hefu, *J. Organomet. Chem.* **1993**, *447*, 227–231; g) L. D. Field, W. J. Shaw, P. Turner, *Organometallics* **2001**, *20*, 3491–3499; h) J. Cámpora, I. Matas, P. Palma, E. Álvarez, C. Graiff, A. Tiripicchio, *Organometallics* **2007**, *26*, 3840–3849; i) K.-E. Lee, X. Chang, Y.-J. Kim, H. S. Huh, S. W. Lee, *Organometallics* **2008**, *27*, 5566–5570; j) S. H. Bertz, Y. Moazami, M. D. Murphy, C. A. Ogle, J. D. Richter, A. A. Thomas, *J. Am. Chem. Soc.* **2010**, *132*, 9549–9551.
[19] K. Itoh, I. Matsuda, F. Ueda, Y. Ishii, J. A. Ibers, *J. Am. Chem. Soc.* **1977**, *99*, 2118–2126.
[20] L. T. Scharf, A. Kowsari, T. Scherpf, K.-S. Feichtner, V. H. Gessner, *Organometallics* **2019**, *38*, 4093–4104.
[21] T. K. N. Kuhn, *Synthesis* **1993**, 561–562.
[22] M. R. Elsby, J. Liu, S. Zhu, L. Hu, G. Huang, S. A. Johnson, *Organometallics* **2019**, *38*, 436–450.
[23] a) G. M. Sheldrick, *SADABS*, Bruker AXS, Madison, USA **2007**; b) *CrysAlisPro, Scale3 Abspack*, Rigaku Oxford Diffraction **2019**.
[24] R. C. Clark, J. S. Reid, *Acta Crystallogr. Sect. A* **1995**, *51*, 887–897.
[25] G. M. Sheldrick, *Acta Crystallogr. Sect. A* **2015**, *71*, 3–8.
[26] O. V. Dolomanov, L. J. Bourhis, R. J. Gildea, J. A. K. Howard, H. Puschmann, *J. Appl. Crystallogr.* **2009**, *42*, 339–341.
[27] G. M. Sheldrick, *Acta Crystallogr. Sect. C* **2015**, *71*, 3–8.
[28] G. M. Sheldrick, *Acta Crystallogr. Sect. A* **2008**, *64*, 112–122.
[29] Deposition Numbers 2127339 (for **1**), 2127345 (for **2**), 2127340 (for **3a**), 2127343 (for **3b**), 2127341 (for **3c**), 2127342 (for **4**), 2127344 (for **5**), and 2127338 (for **6**) contain the supplementary crystallographic data for this paper. These data are provided free of charge by the joint Cambridge Crystallographic Data Centre and Fachinformationszentrum Karlsruhe Access Structures service www.ccdc.cam.ac.uk/structures.

Manuscript received: December 8, 2021
Revised manuscript received: February 12, 2022
Accepted manuscript online: February 14, 2022